

Observation of Vacuum Tunneling of Spin-Polarized Electrons with the Scanning Tunneling Microscope

R. Wiesendanger and H.-J. Güntherodt

Institute of Physics, University of Basel, Klingelbergstrasse 82, CH-4056 Basel, Switzerland

G. Güntherodt

II. Institute of Physics, Rheinisch-Westfälische Technische Hochschule Aachen, D-5100 Aachen, Federal Republic Germany

R. J. Gambino and R. Ruf

IBM T. J. Watson Research Center, Yorktown Heights, New York 10598

(Received 27 March 1990)

Vacuum tunneling of spin-polarized electrons from a ferromagnetic CrO₂ tip into a Cr(001) single crystal has been observed by means of a scanning tunneling microscope (STM) operated in UHV. Topographic STM images of the Cr(001) surface using a tungsten tip confirm the model of topological antiferromagnetism between ferromagnetic terraces separated by monatomic steps of 0.144-nm height. With CrO₂ tips, the measured step-height values alternate around the mean value of 0.144 nm due to an additional contribution from spin-polarized-electron tunneling.

PACS numbers: 75.30.Pd, 61.16.Di, 75.25.+z, 75.50.Ee

Over the past two decades, a number of experimental techniques has been developed to investigate surface magnetism, such as spin-polarized (SP) field emission, SP photoemission, SP tunneling, electron-capture spectroscopy, SP-LEED, Lorentz microscopy, scanning electron microscopy with polarization analysis (SEMPA), and, more recently, magnetic force microscopy (MFM).¹ These techniques can be used, for instance, to measure the spin polarization averaged over surface regions determined by the spatial extension of the probe, to investigate magnetic domain structures, and to probe spin-dependent energy states. Although some of the above-mentioned experimental techniques, such as SEMPA or MFM, simultaneously offer a high spatial resolution of the order of 10 nm, an experimental tool probing real-space magnetic structures down to the atomic scale has not been demonstrated. Since the invention of scanning tunneling microscopy² (STM), which allows the determination of real-space atomic structures, the question arose whether this technique can also be made sensitive to the electron spin and therefore to magnetic structures on the atomic scale. It has already been shown that SP secondary electrons, generated by STM in the field-emission mode, may be used in the future for magnetic imaging on a nanometer scale³ and that a direct observation of the precession of individual paramagnetic spins on oxidized silicon surfaces is possible by STM.⁴ However, evidence has not yet been obtained for tunneling of SP electrons in a STM experiment, offering the opportunity to investigate real-space magnetic structures down to the atomic scale. In contrast to SP tunneling studies using planar tunneling junctions, which can either be superconductor-oxide-ferromagnet junctions⁵ or ferromagnet-oxide-ferromagnet junctions,⁶ the STM technique promises to allow the determination of the local

spin polarization. Here, we report on the first vacuum tunneling experiments of SP electrons from ferromagnetic CrO₂ tips into a Cr(001) surface by means of a STM. We first show that topographic STM measurements performed with a tungsten tip on the Cr(001) surface support the microscopic model by Blügel, Pescia, and Dederichs⁷ of topological antiferromagnetism between ferromagnetic terraces separated by single steps. After replacing the tungsten tip by a ferromagnetic CrO₂ tip, a characteristic alternation of the measured monatomic step-height values is observed which we attribute to an additional contribution from SP tunneling. An expression is derived relating the spin polarization with quantities directly measurable with the STM.

The experiments were performed in a multichamber UHV system (Nanolab) with several surface preparation and analysis facilities.⁸ The pressure in the STM chamber was 1×10^{-11} mbar during all the STM studies reported in this Letter. The calibration of the STM scanning unit was performed laterally by imaging the Si(111)- 7×7 (Ref. 9) and the Si(001)- 2×1 (Ref. 10) surface structures and perpendicular to the surface by imaging monatomic steps on the Si(001)- 2×1 surface. It is important for our analysis of the step structure of the Cr(001) surface that a clear distinction between monatomic and biatomic steps can be made by comparing with the step-height values found on the Si(001)- 2×1 surface. On this surface, monatomic steps separate terraces with the dimer rows oriented at 90° relative to each other, whereas a parallel orientation of the dimer rows is observed on terraces separated by biatomic steps. The noise level of the STM instrument is well below 0.01 nm, which has been proved by imaging the atomic structure of the hexagonally close-packed Au(111) surface with a measured corrugation of the order of 0.02 nm.⁸

All STM data presented in this Letter represent raw data.

For comparison of STM studies with nonmagnetic and magnetic probes, we used electrochemically etched tungsten tips and ferromagnetic CrO_2 tips, respectively. These CrO_2 tips were obtained by first growing 1- μm -thick CrO_2 films with in-plane magnetization on Si(111) substrates covered with a 35-nm-thick TiO_2 nucleation layer. The CrO_2 was deposited by decomposing CrO_3 vapor on a heated substrate in a convection reactor operated in ambient air. The Si(111) substrates were scribed and cleaved on (111) planes after the deposition of the CrO_2 films. The cleavage cracks propagate through the brittle CrO_2 film to give a tip shape at the intersection of particular cleavage planes. The Si substrate at the front end of each tip is etched back in HF-HNO_3 solution which preferentially dissolves the silicon. The overhanging CrO_2 film is used as a magnetic probe. The films have a large remanent magnetization ($\sim 90\%$ of saturation) so the tip is likely to be in a single domain, saturated state. The in-plane magnetization of the CrO_2 films together with the shape anisotropy of the tip lead to a preferred magnetization direction perpendicular to the sample surface in the STM experiment. Recent spin-resolved photoemission experiments on similar ferromagnetic CrO_2 films showed a spin polarization of nearly 100% for binding energies near 2 eV below the Fermi level E_F .¹¹ The large value of the spin polarization may be explained by a spin-filter effect of CrO_2 as a conjectured half-metallic ferromagnet¹² or a more semiconductorlike ferromagnet.¹¹ The CrO_2 tips were therefore favored for SP tunneling experiments with the STM, although they could not so far be prepared as sharp as electrochemically etched tungsten tips.

Apart from the problem of choosing the appropriate SP electron source, a magnetic test structure was needed. We have chosen the Cr(001) surface for the following reason. Recently, Blügel, Pescia, and Dederichs⁷ showed on the basis of self-consistent total-energy calculations that topological antiferromagnetism between ferromagnetic terraces separated by single steps (Fig. 1) is the energetically most favorable structure of this surface. This topological antiferromagnetism of the Cr(001) surface is

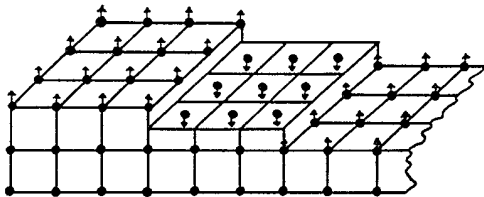


FIG. 1. Topological antiferromagnetic order of the Cr(001) surface with terraces separated by monatomic steps. Different terraces are magnetized in opposite directions. Only surface spins are indicated. (Figure taken from Ref. 7.)

compatible with both the absence of magnetization observed by spin-resolved photoemission¹³ which arises from the cancellation between oppositely magnetized terraces within the diameter of the light spot, as well as with the existence of spin-split surface states detected by energy- and angle-resolved photoemission¹⁴ which are due to majority- and minority-spin states inside each ferromagnetic terrace. The topological antiferromagnetism of the Cr(001) surface with terraces alternately magnetized in opposite directions provides an ideal test structure for SP-STM experiments.

Our topographic STM studies of the Cr(001) surface also strongly support this microscopic model with terraces separated predominantly by monatomic steps [Fig.

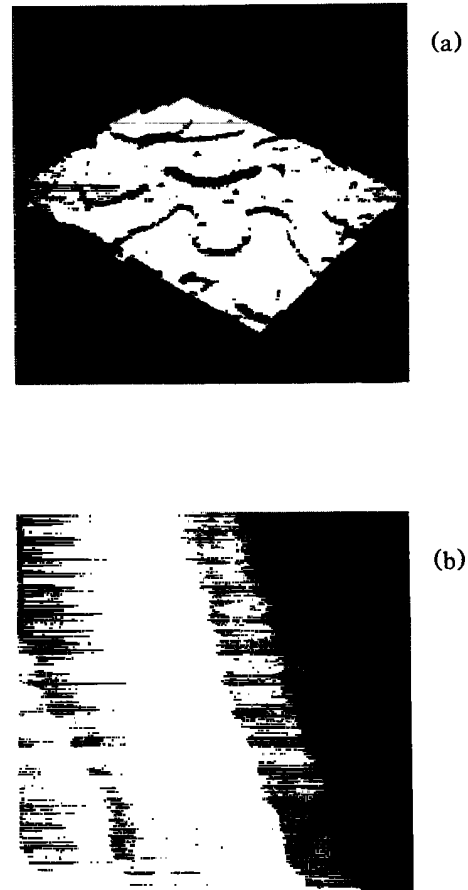


FIG. 2. (a) Constant-current STM image (perspective view) of the Cr(001) surface (128 nm)² obtained with a tungsten tip. Terraces separated predominantly by monatomic steps can be seen. A screw dislocation appears in the upper right-hand part of the image. (Tunneling current $I=1 \text{ nA}$, sample bias voltage $U=+0.05 \text{ V}$.) (b) Constant-current STM image (top view) of the Cr(001) surface (32 nm)² obtained with a CrO_2 tip showing again terraces separated by monatomic steps with different gray levels for each terrace. (Tunneling current $I=1 \text{ nA}$, sample bias voltage $U=+2.5 \text{ V}$.)

2(a)]. The mechanically and electrolytically polished Cr(001) surface was prepared *in situ* over a time period of several months by cycles of Ar⁺-ion etching and annealing. A $p(1 \times 1)$ LEED pattern was obtained, characteristic of a clean Cr(001) surface.¹⁴ Only small traces of oxygen and nitrogen could be detected by x-ray photoelectron spectroscopy. The average width and shape of the observed terraces were found to depend on the annealing conditions, whereas the preferred occurrence of monatomic steps was independent of the preparation conditions. The experimental determination of the monatomic step-height value yields 0.149 ± 0.008 nm, in good agreement with half of the cubic unit-cell height of 0.144 nm for bcc Cr.

After replacing the tungsten tip by a CrO₂ tip, the STM images of the Cr(001) surface showed qualitatively the same topographic structures, i.e., terraces separated by monatomic steps [Fig. 2(b)]. Surprisingly, these monatomic steps could still be imaged with a remarkably high spatial resolution, although the CrO₂ tips appear macroscopically rather blunt. However, we find two different experimental results with CrO₂ tips compared to tungsten tips.

First, a positive sample bias voltage of at least 2 V had to be applied in order to get a stable tunneling current of 1 nA. The I vs V characteristics, which were recorded to investigate the bias-voltage dependence in more detail,

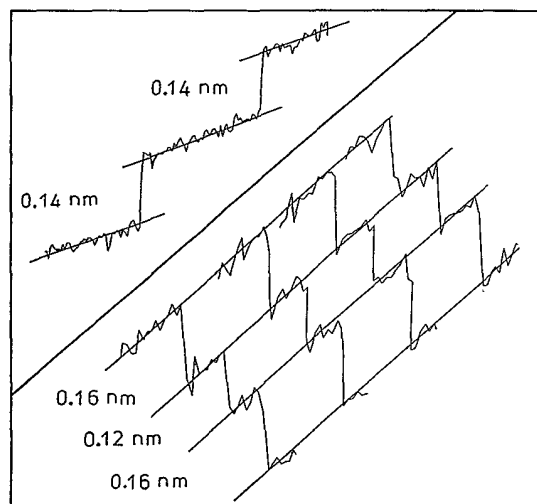


FIG. 3. Arbitrarily chosen (not successive) single-line scans over the same three monatomic steps taken from the STM image of Fig. 2(b), which was obtained with a CrO₂ tip. The same alternation of the step-height values (0.16, 0.12, and again 0.16 nm) in all single-line scans is evident. The line scans are 22 nm long. Inset: For comparison, a single-line scan over two monatomic steps taken from the STM image of Fig. 2(a), which was obtained with a tungsten tip. In this case, the measured step-height value is constant and corresponds to the topographic monatomic step height. This line scan is 70 nm long.

showed the typical appearance of semiconductor-vacuum-metal tunneling rather than that for metal-vacuum-metal tunneling. This observation is consistent with results from spin-resolved photoemission from similar CrO₂ films showing low intensity in the photoemission spectra near E_F .¹¹ We therefore operated the STM always in a regime of maximum spin polarization of the CrO₂, which is found at about 2 eV below E_F .¹¹

Second, a periodic alternation of the measured monatomic step heights between larger and smaller values compared to the mean single step-height value of 0.144 nm is observed (Fig. 3). To support this experimental result, we have analyzed the step heights from individual line scans of over twenty STM raw data images obtained in the constant-current mode. Care was taken to analyze only measured line scans (line scans in the x or y direction) and not oblique line scans where the exactness of the determination of the step-height values can suffer from the interpolation procedure necessary to get the topographic height values along these oblique line scans. It should be noted that the step-height values determined from topographic STM images might sometimes fluctuate within a few percent; however, a periodic alternation of the step-height values, as reproducibly observed in different line scans (independent measurements) with the CrO₂ tip on the Cr(001) surface, has never been found in topographic STM images measured with a tungsten tip. Furthermore, the deviation from the single step-height value determined with a CrO₂ tip can be as large as $\pm 15\%$ which is outside the range of scatter of the monatomic step-height values measured with a tungsten tip. Therefore, we conclude that the observed periodic alternation of the single step-height values is characteristic for STM experiments performed with CrO₂ tips on a Cr(001) surface.

We interpret this periodic alternation of the monatomic step-height values as being due to an additional contribution from SP tunneling. Assume, as sketched in Fig. 4, that the CrO₂ tip is first scanning over a terrace having the same direction of magnetization as the front part

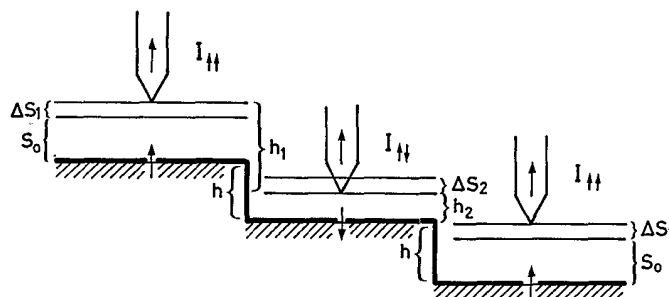


FIG. 4. Schematic drawing of a ferromagnetic tip scanning over alternately magnetized terraces separated by monatomic steps of height h . An additional contribution from SP tunneling leads to alternating step heights $h_1 = h + \Delta S_1 + \Delta S_2$ and $h_2 = h - \Delta S_1 - \Delta S_2$.

of the CrO₂ tip. The tunneling current $I_{\uparrow\uparrow}$ will then be increased due to a contribution from SP tunneling:⁶

$$I_{\uparrow\uparrow} = I_0(1 + P), \quad (1)$$

where I_0 would be the tunneling current without this contribution and P is the effective spin polarization of our tunneling junction. Since the STM is operated at constant current, an additional contribution to the tunneling current leads to a corresponding increase Δs_1 of the mean distance s_0 between the tip and the sample surface. If the CrO₂ tip is scanning over a terrace having the opposite direction of magnetization, the tunneling current $I_{\uparrow\downarrow}$ will be decreased:

$$I_{\uparrow\downarrow} = I_0(1 - P), \quad (2)$$

leading to a corresponding decrease Δs_2 of the distance between tip and sample. The measured single step-height values therefore alternate between $h_1 = h + \Delta s_1 + \Delta s_2$ and $h_2 = h - \Delta s_1 - \Delta s_2$, where h is the topographic monatomic step height. The relationship between

$$P = \frac{I_{\uparrow\uparrow} - I_{\uparrow\downarrow}}{I_{\uparrow\uparrow} + I_{\uparrow\downarrow}} \quad (3)$$

and $\Delta s_1, \Delta s_2$ is given by

$$P = \frac{\exp(A\sqrt{\phi}\Delta s_1) - \exp(-A\sqrt{\phi}\Delta s_2)}{\exp(A\sqrt{\phi}\Delta s_1) + \exp(-A\sqrt{\phi}\Delta s_2)} \\ = \frac{\exp(A\sqrt{\phi}\Delta s) - 1}{\exp(A\sqrt{\phi}\Delta s) + 1}, \quad (4)$$

where ϕ is the mean local tunneling barrier height, $\Delta s = \Delta s_1 + \Delta s_2$, and $A \approx 1 \text{ eV}^{-1/2} \text{ \AA}^{-1}$. Equation (4) represents a relationship between the effective spin polarization P and the quantities ϕ and Δs which are directly measurable with the STM. Apart from the determination of the changes of the single step-height value, measurements of ϕ are necessary to derive P . We have determined ϕ from the slope of local $\ln I$ vs s characteristics. The value of ϕ lies between 3 and 5 eV for all of over one hundred $\ln I$ vs s characteristics which were measured with different sample bias voltages between +2.5 and +3.5 V. These ϕ values indicate that clean conditions for the tip and the sample surface were achieved, whereas anomalous low ϕ values were reported for contaminated surfaces of either tip or sample.¹⁵ Therefore, we have confidence that the derived values for the polarization P cannot greatly be affected by surface contamination. Taking $\Delta s = 0.02 \pm 0.01 \text{ nm}$ and an average value of $4 \pm 0.5 \text{ eV}$ for ϕ , we derive values for P of $(20 \pm 10)\%$. The tip-to-sample distance at 1-nA tunneling current and a sample bias voltage of +2.5 V was determined to be about 0.5 nm. Measuring the distance and the bias-voltage dependence of the local spin polarization will both be interesting topics for future investigations.

In summary, we have demonstrated that SP tunneling can be detected and the local spin polarization P can be determined by the STM using ferromagnetic CrO₂ tips.

This opens the door for studies of magnetic structures on the atomic scale by STM. Improvements in the sharpness of the ferromagnetic probing tips might lead, for instance, to the first real-space images of in-plane antiferromagnetic structures in the future.

We would like to thank Professor H. Thomas for many stimulating discussions, Professor A. Hubert for electropolishing the Cr(001) single crystal, D. Bürgler and G. Tarrach for their assistance and comments on the manuscript, as well as H. Breitenstein, H. R. Hidber, P. Reimann, R. Schnyder, and A. Tonin for their technical help. Financial support from the Swiss National Science Foundation and the Kommission zur Förderung der wissenschaftlichen Forschung is gratefully acknowledged.

¹For recent reviews of spin-polarized probes, see R. J. Celotta and D. T. Pierce, *Science* **234**, 334 (1986); M. Landolt, *Appl. Phys. A* **41**, 83 (1986); J. Kirschner, *Polarized Electrons at Surfaces* (Springer-Verlag, Berlin, 1985); C. Rau, *J. Magn. Mater.* **30**, 141 (1982); R. Feder, *J. Phys. C* **14**, 2049 (1981).

²G. Binnig, H. Rohrer, Ch. Gerber, and E. Weibel, *Phys. Rev. Lett.* **49**, 57 (1982).

³R. Allenspach and A. Bischof, *Appl. Phys. Lett.* **54**, 587 (1989).

⁴Y. Manassen, R. J. Hamers, J. E. Demuth, and A. J. Castellano, Jr., *Phys. Rev. Lett.* **62**, 2531 (1989).

⁵P. M. Tedrow and R. Meservey, *Phys. Rev. Lett.* **26**, 192 (1971).

⁶M. Julliere, *Phys. Lett.* **54A**, 225 (1975); S. Maekawa and U. Gäfvert, *IEEE Trans. Magn.* **18**, 707 (1982); J. C. Slonczewski, *J. Phys. (Paris), Colloq.* **49**, C8-1629 (1988).

⁷S. Blügel, D. Pescia, and P. H. Dederichs, *Phys. Rev. B* **39**, 1392 (1989).

⁸R. Wiesendanger, G. Tarrach, D. Bürgler, T. Jung, L. Eng, and H.-J. Güntherodt, in *Proceedings of the Eleventh International Vacuum Congress and Seventh International Conference on Solid Surfaces*, Cologne, West Germany, 1989 [Vacuum (to be published)]; R. Wiesendanger, D. Bürgler, G. Tarrach, D. Anselmetti, H. R. Hidber, and H.-J. Güntherodt, in *Proceedings of the International Conference on Scanning Tunneling Microscopy, Oarai, Japan, 1989* [*J. Vac. Sci. Technol. A* **8**, 339 (1990)].

⁹R. Wiesendanger, G. Tarrach, D. Bürgler, and H.-J. Güntherodt, *Europhys. Lett.* **12**, 57 (1990).

¹⁰R. Wiesendanger, D. Bürgler, G. Tarrach, and H.-J. Güntherodt, *Surf. Sci.* (to be published).

¹¹K. P. Kämper, W. Schmitt, G. Güntherodt, R. J. Gambino, and R. Ruf, *Phys. Rev. Lett.* **59**, 2788 (1987).

¹²K. Schwarz, *J. Phys. F* **16**, L211 (1986).

¹³F. Meier, D. Pescia, and T. Schriber, *Phys. Rev. Lett.* **48**, 645 (1982).

¹⁴L. E. Klebanoff, S. W. Robey, G. Liu, and D. A. Shirley, *Phys. Rev. B* **30**, 1048 (1984); L. E. Klebanoff, R. H. Victora, L. M. Falicov, and D. A. Shirley, *Phys. Rev. B* **32**, 1997 (1985).

¹⁵J. H. Coombs and J. B. Pethica, *IBM J. Res. Dev.* **30**, 455 (1986).